Space vector control for multilevel static synchronous compensator in wind energy systems

Gundala Muni Reddy[1], Ammapalli Hema Sekhar[2], Selika Narasimha Rao[1], Kuruna Divakar[1], Kola Murali Kumar[1], Nathella Munirathanm Giri Kumar[3], Gunti Kishor Babu[4], Vayyala Jyothsna Priya[1]

[1]Department of Electrical and Electronics Engineering, Siddharth Institute of Engineering and Technology, Puttur, India
[2]Department of Electrical and Electronics Engineering, VEMU Institute of Technology, Kothakota, India
[3]Department of Electrical and Electronics Engineering, Sir M. Visvesvaraya Institute of Technology, Bengaluru, India
[4]Department of Electrical and Electronics Engineering, Kallam Haranadhareddy Institute of Technology, Guntur, India

Article Info

Article history:

Received Aug 24, 2025
Revised Jun 17, 2026
Accepted Aug 13, 2026

Keywords:

Multilevel inverter
Simple hysteresis current controller
Space vector hysteresis current controller
Static synchronous compensator
Wind energy system

ABSTRACT

To meet the higher demand for energy, fossil fuels have been the leading energy source. These fuels produce greenhouse gases (GHG) and these gases are the reason for climate change, and the fossil fuel resources are also running out quickly. Because of this, lawmakers need to switch to clean and renewable energy sources, including solar, geothermal, wind, tidal, and biomass. The wind energy industry has developed a lot because of new technologies, which has led to more wind turbines (WTs) being connected to the grid. Integrating a lot of WTs into the grid has caused challenges like power quality (PQ), grid stability, and reactive power correction. This study utilizes a multilevel inverter-based static synchronous compensator (STATCOM) with a space vector hysteresis current controller (SVHCC) to mitigate the impacts of WTs. The proposed control strategy improves PQ by reducing total harmonic distortion (THD) and maintaining unity power factor (UPF) even in the presence of nonlinear load and induction generator (IG). The desired results are obtained with a lower switching frequency, thereby improving efficiency and reducing stress on power electronic devices. The proposed SVHCC-based STATCOM is modelled and evaluated using MATLAB/Simulink, and its performance is compared with both uncompensated system and a simple hysteresis current controller (SHCC)-based STATCOM.

Corresponding Author:

Gundala Muni Reddy
Department of Electrical and Electronics Engineering, Siddharth Institute of Engineering and Technology
Puttur, India
Email: munireddyg@gmail.com

1. INTRODUCTION

Modern human beings harness energy from various sources to meet all the needs of their daily activities. The assessment of the energy consumption of a country can provide us with information about the economic development and standards of living of its people. Rapidly developing nations are trying to lift the people out of poverty, and this causes the people to have a better quality of life, leading to increased energy demand. As per the prediction of the International Energy Agency (IEA), the population of the world will increase to 9 billion in 2040, and the increased population leads to increased energy demand. A growing economy, rapid urbanization, and technological advancements also contribute to the increasing demand for energy [1]. In the year 2017, the share of fossil fuels in the world's energy sector is about 70%, and this predominant contribution to the energy sector by fossil fuels is due to availability of infrastructure and the fact that fossil fuel technology is well mature [2]. But the scenario for fossil fuels is quickly shifting due to the emission of greenhouse gases (GHG) and the effects of GHG on the global environment. Fossil fuels are being used globally; generation alone is one-third of total global GHG production. This triggered a change in climate, and this further caused a change in global ecological balance [3].

In view of changing climate and its consequences on life on Earth, global leaders signed an agreement at the United Nations (UN) climate change conference in Paris to limit the average global increase in temperature to under 2 °C above pre-industrial levels by 2,100. The exact estimates of fossil fuel reserves on Earth are not known, but there are some estimates that, with the present rate of usage and production, crude oil may completely deplete in 50 years, coal may deplete in 300 years, and other fossil fuels may deplete in between these two extremes [4]. Due to these factors, policymakers are designing policies in the energy sector to encourage usage of renewable energy. As per the reports of the World Energy Council (WEC), the global energy demand will reach its peak value in 2030 [5]. Hence, policymakers are worried about meeting this increased demand with uncertain and GHG-emitting fossil fuels. All these factors triggered rapid growth in the renewable energy sector and, in particular, wind energy. As per the reports of the IEA, wind energy has increased by a record value of 273 terawatt-hours (TWh) in 2021, which is 55% more in comparison to the growth achieved in 2020, and it was the highest growth recorded among all energy sources in renewable energy sector [6]. As per the Global Wind Report–2022 of the Global Wind Energy Council (GWEC), global wind energy capacity is 837 GW in 2022, which serves a reduction of 1.2 billion tons of CO_2 annually, which is equivalent to the annual CO_2 emissions of South America [7].

During the times when wind energy production was a small amount and it was in the development stage, there were no stringent rules for the generation of wind energy and its grid integration. The rules were a bit liberal in the early days of wind energy generation so as to encourage wind energy generation [8]. Moreover, in the early days, the grid integration of wind energy was a small amount in comparison with traditional sources, and its integration into the grid did not pose great challenges. Normally, the wind energy system (WES) is equipped with an induction generator (IG), which is cheaper and rugged in construction, requiring little maintenance. But the characteristics of IG are different from those of the alternators employed in traditional power plants. Due to the disparity of characteristics between traditional alternators and IG, bulk wind power generation and its integration into the grid comprising conventional alternators pose challenges like grid stability and power quality (PQ) issues [9]. Due to these factors, electrical utilities are considering wind energy as a risky source for grid integration and are more concerned about PQ and grid stability.

Mahela *et al.* [10] have proposed Stockwell's transform (ST)-based algorithm for analyzing PQ issues in grid-integrated WESs for various operating conditions. The current and voltage measurements have been done using PQ analyzer available with WTviewer software. The various signals are analyzed using ST to identify different PQ issues. Almohaimeed and Akher [11] have focused on issues like short-duration voltage changes and harmonics due to the integration of wind energy. This paper also focused on solutions to overcome above-said problems in grid-integrated WES. This paper has concentrated more on PQ issues like voltage variations, as it is more severe, and case studies have been presented on this issue. Ravi *et al.* [12] have studied various issues present in grid integration of solar and wind energy and proposed a fuzzy logic controller (FLC)-based interline unified power quality conditioner (UPQC) to mitigate the PQ issues. The study also highlighted through a literature survey that the dynamic voltage restorers (DVRs) are suitable for rapid correction in voltage sags and swells to ensure a stable power supply. The reliability and harmonics mitigation can be effectively done by energy storage systems (ESS). The study showed that FLC-based interline UPQC has effectively addressed PQ issues like voltage and current variations and harmonics. Vineeth *et al.* [13] have proposed a multi-converter (MC)-UPQC for mitigating PQ issues in grid-integrated renewable energy systems. The proposed system with MC-UPQC helps to mitigate current and voltage issues simultaneously in multi-bus or multi-feeder systems. This proposed method helps in mitigating PQ issues and other issues caused by switching of capacitor banks and lightning strikes.

Chahine *et al.* [14] have proposed a model-based technique called the matrix pencil method for the generation of reference currents. The effectiveness of the suggested method is analyzed for reduction in current harmonics and better power factor for different modulation schemes. The proposed method's performance is analyzed by comparing it with the results obtained with two methods, namely synchronous reference frame theory (SRFT) and instantaneous reactive power theory (IRPT). The results have proved that the proposed method has lower total harmonic distortion (THD) in source currents and faster response in comparison with IRPT and SRFT. Magesh *et al.* [15] have developed a wind turbine (WT) model and its control strategy using DIgSILENT software. The control strategies are developed for both generator-side and grid-side converters to ensure PQ in the WES. Various circumstances have been simulated to study the PQ issues and the effectiveness of the suggested control scheme. To reduce the complexity of the wind farm model, an aggregate model of each wind farm feeder has been used. Shao *et al.* [16] have presented a detailed review of various challenges in maintaining PQ of offshore wind energy grid integration. This paper also provided insight into challenges and future directions of research in algorithms, frameworks, and measurements. The survey presented in this paper facilitated a deeper understanding by further exploring root causes of PQ issues and then discussing the emerging algorithmic solutions for mitigating PQ issues in grid integration of wind energy. Pan *et al.* [17] have employed a modulated model-predictive control (MMPC) strategy for modular multilevel cascaded converter (MMCC)-based static synchronous compensators (STATCOMs) to adjust imbalanced load current and manage reactive power flow. By adding a common-mode voltage (CMV) to the phase voltages of the star-connected MMCC current model, the approach allows for the natural injection of a nonsinusoidal voltage into the converter's neutral point, resulting in interphase cluster voltage balancing.

Martín *et al.* [18] recommends an energy storage STATCOM model with grid-forming control as a feasible alternative to rotating synchronous condensers (RSC) for enhancing grid access capacity for integration of renewable energy. To assure system stability, a control approach based on the synchronous machine swing equation is proposed, along with a power system stabilizer (PSS). The PSS addresses the oscillatory response that occurs while replicating the behavior of the RSC in the converter. Benevieri *et al.* [19] have given an overview of classification, major topologies, recent advances, and emerging directions of multilevel converter technology. Researchers and engineers can learn a lot about how to design, improve, and use multilayer converter technology by looking into its past and future research areas. Yeboah *et al.* [20] look at different ways to add renewable energy to smart grids. These include better systems for control and protection, smart systems for storing and managing energy, upgrades to the grid's infrastructure, and the making of predictive models. The results show issues and problems, such as grid instability and intermittent renewable energy supplies. The study demonstrates the significance of developing hybrid optimization models to enhance load scheduling, peak shaving, and cost reduction. The literature review above shows that people have looked into different issues with PQ. The controller suggested in this paper will meet the required PQ standards by lowering the frequency at which power electronic switches switch.

To address the concerns of electrical utilities, the International Electrotechnical Commission (IEC) recommended the draft IEC-61400-21 standard for grid integration of wind energy in 1995, and in 2001, the IEC published the first edition of IEC-61400-21. The IG is simple, rugged in construction and economical, but it takes reactive power from the supply for its operation, burdening the grid to provide reactive power to the IG as well as the load. This causes a reduction in power factor at the source, leading to the introduction of some equipment for power factor correction [21]. The intention of the suggested control strategy is to provide reactive power to both the nonlinear resistive-inductive load (R-L) and the IG and therefore maintain unity power factor (UPF) at the source. The proposed control scheme produces currents in such a way as to nullify the effects of harmonics introduced by nonlinear load, therefore maintaining THD in the grid-connected WES at the prescribed levels. Another objective of the space vector hysteresis current controller (SVHCC) control strategy is to achieve the desired PQ norms at a lower switching frequency for insulated-gate bipolar transistor (IGBT) switches in STATCOM.

The specific contributions made by this research study are as follows. This paper proposes a novel SVHCC control strategy for improving the PQ in grid-connected WESs. This controller shall achieve the desired PQ norms with a lower switching frequency of IGBT switches employed in STATCOM. Maintains UPF at the source even with the presence of nonlinear load and IG. Cancels the harmonics injected by nonlinear load, thus maintaining THD within the prescribed limits. Provides necessary reactive power to nonlinear load and IG, thus reducing the burden on the source.

To highlight the efficiency of SVHCC, a comparative analysis has also been done with simple hysteresis current controller (SHCC), which is a conventional and popular controller. This comparative study will demonstrate the effectiveness of the proposed novel controller for grid-connected WESs. The remaining paper has been structured as follows: section 2 outlines the structure of grid-connected WES. Subsection 2.1 provides the mathematical analysis for the generation of reference currents. Subsection 2.2 explains the concept of simple hysteresis current control. Subsection 2.3 explains the mathematical concepts of SVHCC. Section 3 explains the simulation study carried out in MATLAB, including a comparative analysis between SVHCC and SHCC. Finally, section 4 summarizes the main conclusions of the research study.

2. RESEARCH METHOD

To study the effectiveness of the SVHCC controller in mitigating the PQ issues with the lower switching frequency, a grid-integrated WES is considered, as shown in Figure 1. The proposed system comprises a power supply, STATCOM, WES connected with an IG and a nonlinear load R-L, all connected at the point of common coupling (PCC). The block diagram in Figure 2 shows the details of the control mechanism along with various input and output signals to the control scheme. Load currents

($A = I_{La}{}' I_{Lb}{}' I_{Lc}$), source currents ($I_{sa}{}' I_{sb}{}' I_{sc}$), source voltages ($V_{sa}{}' V_{sb}{}' I_{sc}$), direct current (DC) link capacitor voltage, V_{dc}, and V_{dcref} are various inputs to the control system. The grid voltages are measured for the purpose of grid synchronisation. The control scheme generates reference currents to compare with actual currents for generating switching pulses of the STATCOM.

A WT extracts wind energy, and an IG is coupled to the WT to generate electrical energy from the kinetic energy of wind. In WES, the WT and generator are coupled through a gear mechanism to match the low-speed WT and high-speed generator. The generator normally employed in WES is a three-phase synchronous generator, permanent magnet synchronous generator (PMSG), and IG. PMSG and squirrel cage IGs are most commonly used in WES due to their economy and reliability. As squirrel cage IG is cheaper, simpler, and rugged in construction, no separate DC excitation is required, and it offers natural short-circuit protection; hence, it is employed here in the proposed system [22].

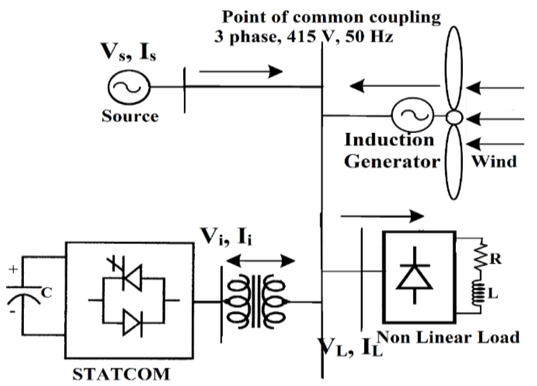

Figure 1. Configuration of the grid-connected WES, with IG, multilevel inverter-based STATCOM

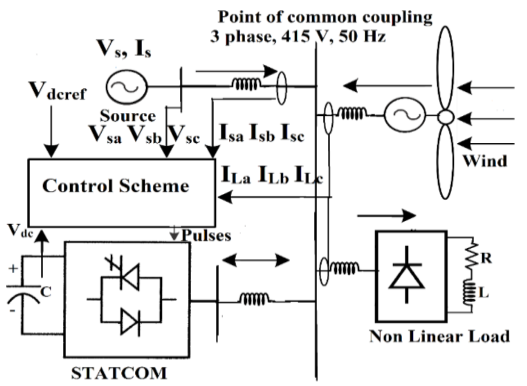

Figure 2. Block diagram of the proposed control strategy for the multilevel inverter-based STATCOM

2.1. Generation of reference currents

A unit template control strategy, which is simple and easily implementable, is employed in this paper to extract reference currents. To obtain the desired PQ norms in the grid-connected WES, the switching pulses are generated for the IGBTs of STATCOM by comparing reference and actual currents. The block diagram representation of the unit template method of generating reference currents is depicted in Figure 3.

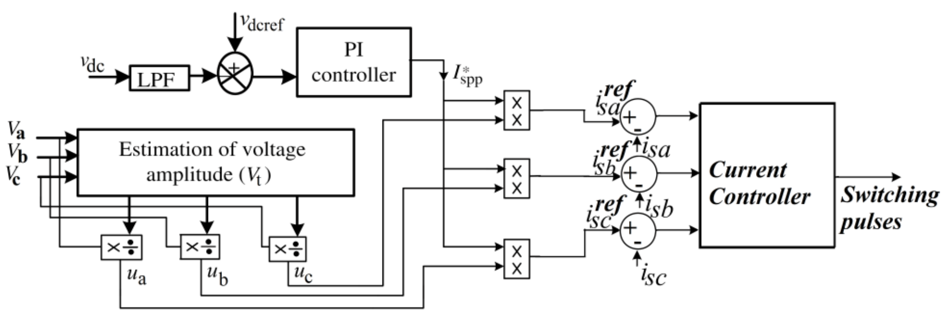

Figure 3. Block diagram showing extraction of reference currents

The 3-Φ voltages, $V_{sa}, V_{sb}\ V_{sc}$, are measured and then v_a, v_b and $v_c$voltages are obtained by filtering $V_{sa}, V_{sb}\ V_{sc}$, voltages. Voltage amplitude, v_t, at PCC, is evaluated as in (1).

$$v_t\{(2/_3)(v_a^2 + v_b^2 + v_c^2)\}^{1/_2} \quad (1)$$

From (1), unity amplitude templates u_a, u_b and u_c are obtained in (2).

$$ua = va/Vt, ub = vb/Vt, uc = vc/Vt \quad (2)$$

Using a low-pass filter, DC link voltage, V_{dc}, is processed, and then a comparison is made with the reference DC link voltage, V_{dcref}. The output of the comparator is processed by the proportional-integral (PI) controller to obtain the reference source current amplitude, I^*_{spp}. On comparing reference and average values of voltages of the DC bus of STATCOM, a voltage error is obtained, which is processed through a PI controller as in (3).

$$v_{dce}(n) = v_{dcref}(n) - v_{dca}(n) \quad (3)$$

The PI controller's output, fed with the voltage error, is in (4).

$$I_{spp}(n) = I_{spp}(n-1) + K_{pd}\,\{v_{dce}\,(n) - v_{dce}\,(n-1)\} + K_{id}v_{dce}(n) \quad (4)$$

K_{pd} is Proportional gain constant and K_{id} is integral gain constant. The supply reference currents are computed as in (5) [23].

$$i_{sa}^{ref} = I^*{}_{spp}.u_a;\ i_{sb}^{ref} = I^*{}_{spp}.u_b;\ i_{sc}^{ref} = I^*{}_{spp}.u_c \quad (5)$$

2.2. Simple hysteresis current controller design

In this research study, SVHCC is employed for the generation of switching pulses in STATCOM. In this research study, STATCOM based on a three-level inverter (TLI) topology with SVHCC is utilized for the grid-connected WES for studying the associated PQ problems. To explore the merits of SVHCC, a comparative study of TLI-based STATCOM for the same grid-connected WES has been performed with the SHCC. First, the details of SHCC for TLI-based STATCOM are provided. SHCC is a popular, conventional, simple, and easily implementable controller. The reference currents as per (5) are compared with the sensed actual currents to obtain the current error. The error thus obtained is fed to SHCC for the generation of switching pulses for IGBTs present in STATCOM to compel the actual currents to stay within the prescribed upper and lower bands around reference currents to achieve the desired PQ characteristics [24], [25]. Figure 4 shows the block diagram to implement SHCC for phase A, and it can be implemented for the remaining phases in a similar way as shown in Figure 4.

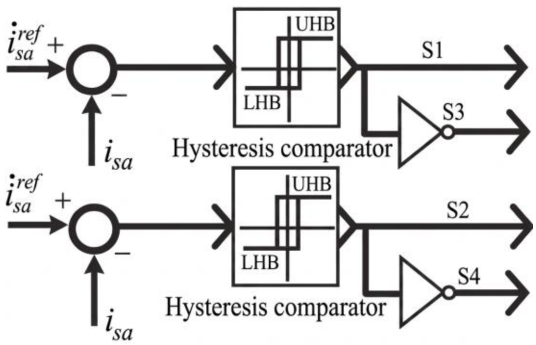

Figure 4. SHCC implementation for phase A to generate switching signals

2.3. Space vector hysteresis current controller design

There are several current controllers proposed in the literature for obtaining the desired current waveform with prescribed THD levels, and among all of them, hysteresis current controllers (HCCs) are popular as these controllers are easy to realize with excellent characteristics of dynamic response. HCCs are classified as two categories: traditional and SVHCC. Traditional HCCs are popular because of features like easy implementability, good dynamic response, limited peak current, and handling of load parameter changes. The HCC is equipped with three independent controllers for three phases of the inverter, thus leading to a lack of coordination among independently controlled HCCs. This lack of coordination causes the current error to remain outside the defined bands around the reference currents, leading to increased distortions in the current waveform and a higher switching frequency of IGBTs in the STATCOM [26], [27].

The problems in the SHCC can be overcome by the SVHCC as control action takes place on the combined effect of current errors in three phases rather than independent control action based on independent controllers in three phases in the SHCC. The transformation of 3-Φ currents and voltages from rotating 3-Φ (a, b, and c) coordinates to a two-phase stationary (α and β) coordinate system has been done in SVHCC to bring coordination among the three phases for a better control strategy. For the analysis of the SVHCC, the concept of a complex space vector is applied, which represents 3-φ quantities with a single space vector. Each phase of a TLI-based STATCOM has four bidirectional switches, Sx1–Sx4, and two clamping diodes Dx1 and Dx2, where x = a, b, and c phases. Various switching states of IGBTs in STATCOM with TLI topology are shown in Table 1. Both capacitors are charged to the DC voltage U_{dc}. Phase voltages of TLI-based STATCOM after transforming into stationary two-phase (α and β) coordinate system from a three-phase (a, b, and c) system are as in (6).

$$\begin{pmatrix} v_\alpha \\ v_\beta \end{pmatrix} = \begin{pmatrix} \frac{2}{3} & \frac{-1}{3} & \frac{-1}{3} \\ 0 & \frac{1}{\sqrt{3}} & \frac{-1}{\sqrt{3}} \end{pmatrix} \begin{pmatrix} v_a \\ v_b \\ v_c \end{pmatrix} \quad (6)$$

Table 1. Switching states of TLI-based STATCOM

S_{1x}	S_{2x}	S_{3x}	S_{4x}	V_{x0}	Switching state
On	On	Off	Off	U_{dc}	P
Off	On	On	Off	0	O
Off	Off	On	On	$-U_{dc}$	N

TLI-based STATCOM shall have 27 switching states and 19 voltage vectors (VV). V_0 is a zero VV; VVs, V1,4,7,10,13,16 are defined as small VVs; VVs, V3,6,9,12,15,18 are defined as medium VVs; and VVs, V2,5,8,11,14,17 are defined as large VVs. A total of 27 switching states and 19 VVs are shown in Figure 5 [28], [29]. The schematic diagram of TLI-based STATCOM with IGBTs and diodes is shown in Figure 6. In SHCC, the controller shall try to keep the actual source currents around the three bands as shown in Figure 7. In the stationary two-phase (α and β) coordinate system, three hysteresis bands for three-phase currents result in a hexagon area as depicted in Figure 8. The three-phase reference currents will give one reference vector in a stationary two-phase (α and β) system, and the tip of this vector moves on a circle in a stationary two-phase (α and β) system. As the reference current is a circle, the hexagon area due to three hysteresis bands will also move on this circle in the (α and β) coordinate system as depicted in Figure 8. The control logic of SVHCC is such that the sensed source current, i, in the stationary two-phase (α and β) system should always be within the hexagon area, which corresponds to keeping the current within the three bands in the three-phase system. As indicated in Figure 8, vector, i_e can be mathematically represented as in (7).

$$i_e = i - i_{ref} \quad (7)$$

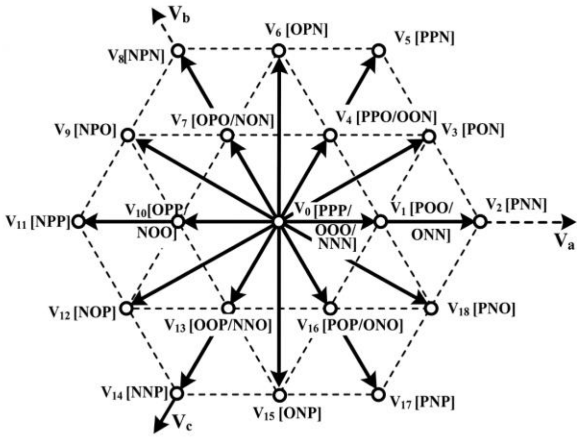

Figure 5. Switching states of TLI-based STATCOM

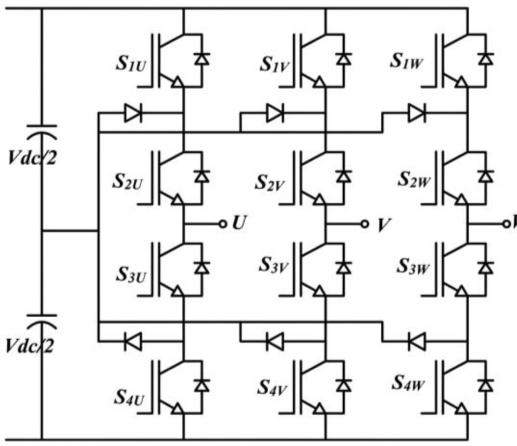

Figure 6. Schematic diagram of TLI-based STATCOM

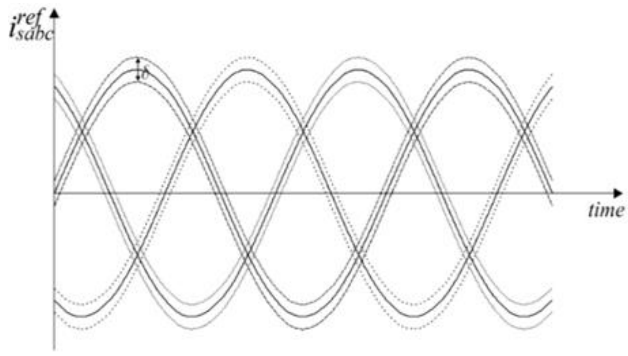

Figure 7. Reference currents with defined hysteresis bands

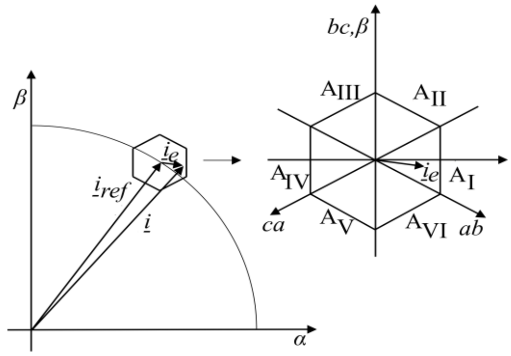

Figure 8. Various currents in stationary α–β system

The reference current, i_{ref} will always be at the centre of the hysteresis hexagon, and the actual current, i, should always be kept in the hysteresis hexagon area so as to obtain the desired PQ norms. This fact implies that the current error vector, i_e, should always be kept in the hysteresis hexagon area so as to obtain desired PQ norms. If the vector, i_e, is present within the hysteresis hexagon area, then there is no need of any control action from STATCOM and thus no change in switching states of STATCOM is needed, and the STATCOM continues to operate in the same switches of STATCOM in ON state. If the current error vector, i_e moves beyond hexagon area, then this indicates that the error is not within the prescribed limits. Now, the switching logic has to decide which VV among the available 19 VVs is to be selected to bring back current error vector into hexagon region.

In some cases, the current error vector may go to a greater extent beyond the hexagon area; for a better response, the vector i_e must be forced back to the hexagon area as quickly as possible. For this purpose, an additional bigger hexagon is placed around the existing one, as shown in Figure 9. For an error vector lying in the stationary hexagon region, there is no need of any control action. For an error vector lying in the region between stationary hexagon and dynamic hexagon, error vector can be moved slowly for lower switching frequency, and hence switching logic is designed using small VVs. To understand the switching logic, let us consider the following illustration. If the error vector is present in region A_{II} then the suitable VV to force the vector, i_e, into hexagon area, will be V_{13}, as this VV is opposite to the region under consideration. With the same logic, we can obtain the switching logic as indicated in Table 2. If an error vector is present in the region outside of the dynamic hexagon, then large and medium VVs are applied to move the error vector quickly back to the inside of the stationary hexagon for a good dynamic response. Table 3 indicates the appropriate switching logic for this case. The block diagram of the control system of SVHCC is shown in Figure 10. The flowchart that explains the various steps of analysis involved in the SVHCC is shown in Figure 11.

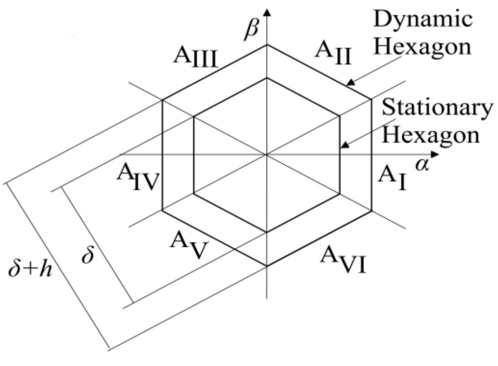

Figure 9. Stationary and dynamic hexagons

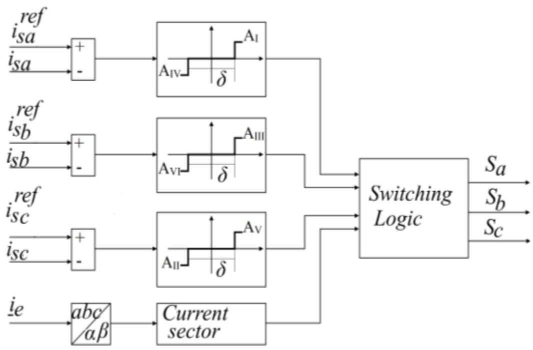

Figure 10. Block diagram of control system of SVHCC

In SHCC, reference currents are defined with hysteresis bands to correct current errors quickly, whereas the SVHCC architecture uses error vectors to take synchronized decisions in the α and β plane. This hybrid structure combines hysteresis control's simplicity and resilience with space vector methods' ability to select vectors optimally. The switching scheme of SVHCC is shown in Tables 2 and 3. This table shows how the controller selects the suitable VV from the available vector set based on the size and direction of the current error vector. The proposed SVHCC employs synchronized multi-phase switching to reduce unnecessary transitions and current ripple. This controller is different from standard SHCC, which switches phases one at a time.

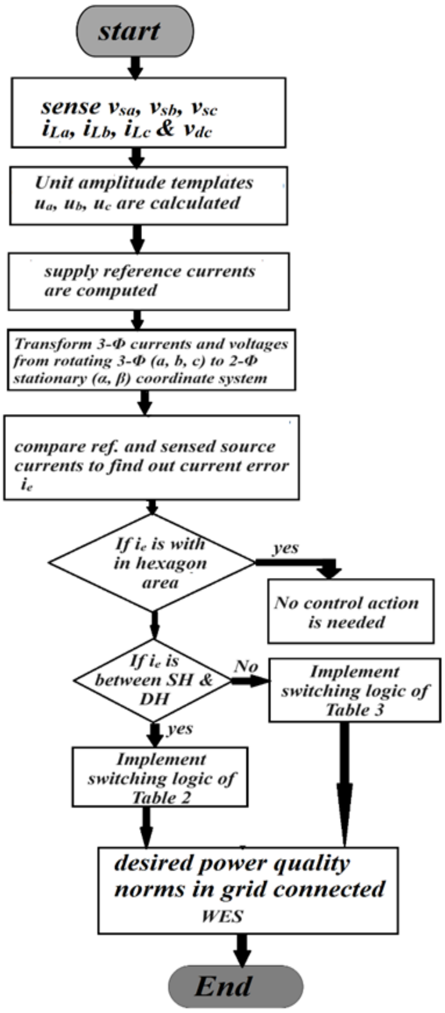

Figure 11. Flow chart showing various steps of analysis of SVHCC scheme

Table 2. Switching table for error vector is present between stationary hexagon and dynamic hexagon

Sector	1	2	3	4	5	6
Error region	A_I	A_{II}	A_{III}	A_{IV}	A_V	A_{VI}
VV	V_{10}	V_{13}	V_{16}	V_1	V_4	V_7

Table 3. Switching table when the error vector is beyond dynamic hexagon

Sector	1	2	3	4	5	6	7	8	9	10	11	12
Error region	-15°-15°	15°-45°	45°-75°	75°-105°	105°-135°	135°-165°	165°-195°	195°-225°	225°-255°	255°-285°	285°-315°	315°-345°
VV	V_{11}	V_{12}	V_{14}	V_{15}	V_{17}	V_{18}	V_2	V_3	V_5	V_6	V_8	V_9

3. RESULTS AND DISCUSSIONS

The WES, with a nonlinear load R-L and a WT-driven IG, shown in Figure 1 is considered for the analysis of PQ with the desired control scheme. The WES is simulated in MATLAB/Simulink for studying

PQ issues due to nonlinear load and IG. The WES is simulated in MATLAB/Simulink with the specifications shown in Table 4 for studying PQ issues due to nonlinear load and IG. Figure 12 displays the MATLAB/Simulink simulation diagram for the system under study. In this study, a comparative analysis is performed on the system shown in Figure 1 to understand the performance of the control scheme in mitigating the PQ issues introduced due to the nonlinear load and IG. First, the system is simulated without any control system incorporated so as to understand the performance of the control system. Later on, the same system is simulated with the SHCC scheme and then with the SVHCC control scheme so as to compare both control schemes and highlight the effectiveness of SVHCC in obtaining the desired PQ norms with lower switching frequencies.

Table 4. System parameters

No	System parameters	Specifications
1	Grid voltage	3-Φ, 415 V, 50 Hz
2	IG	3.5 KVA, 415 V, 50 Hz, P = 4, Speed = 1440 rpm, R_r = 0.1 Ω, R_s = 0.15 Ω, L_s = L_r = 0.06 H
3	Line inductance	0.05 mH
4	Inverter parameters	DC link voltage = 800 V, DC link capacitance = 100 µF
5	IGBT rating	Collector Voltage = 1200 V, forward current = 50 A, gate voltage = 20 V
6	Load	Non-linear load with R = 15 Ω and L = 20 mH

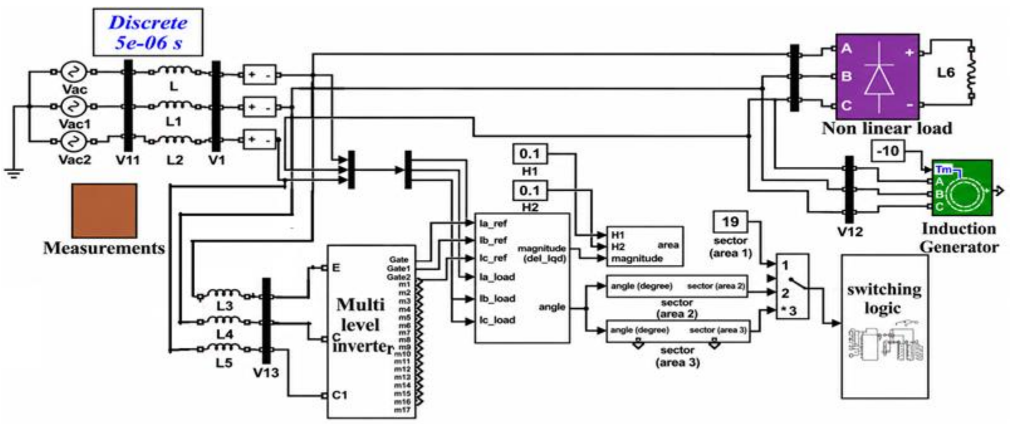

Figure 12. Simulink model of the proposed WES with SVHCC controller

3.1. Analysis of wind energy system without static synchronous compensator

Figure 13 shows the current waveforms of the grid-connected WES in the uncompensated situation, which indicates the effect of the nonlinear load on the system performance. The load current waveform in Figure 13(a) is non-sinusoidal because of the nonlinear load R-L. The matching source current waveform is shown in Figure 13(b), where the remarkable harmonic distortion occurs without STATCOM correction. This distortion is an indication of poor PQ, which is further justified by the high THD value (26.12%) as shown in Figure 14 and reduced power factor, as shown in Figure 15.

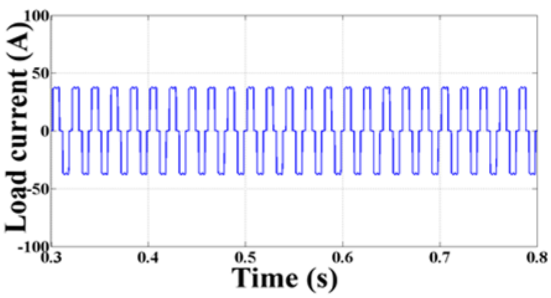

(a)

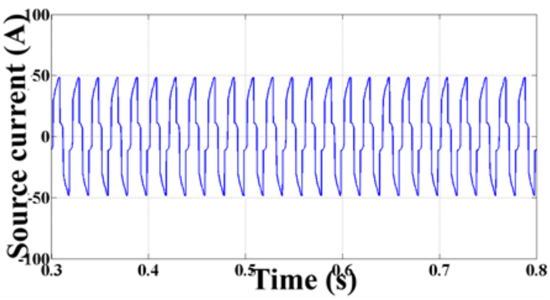

(b)

Figure 13. Current waveforms of the grid-connected WES without STATCOM: (a) nonlinear load current waveform showing non-sinusoidal nature and (b) source current waveform exhibiting harmonic distortion

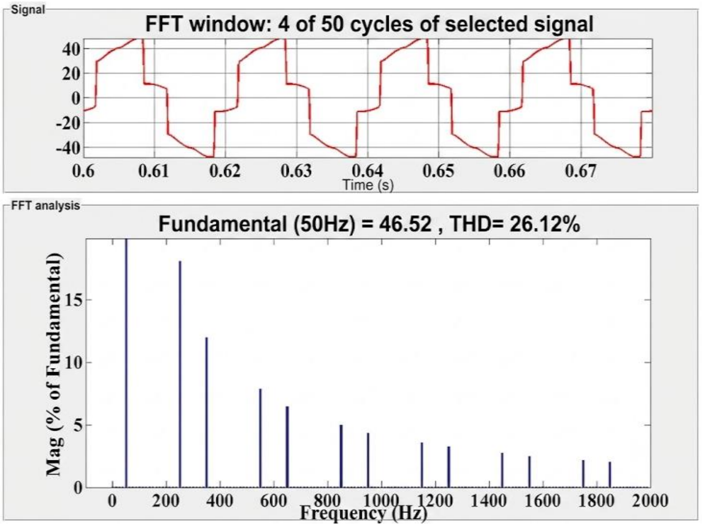

Figure 14. THD value of source current without compensation

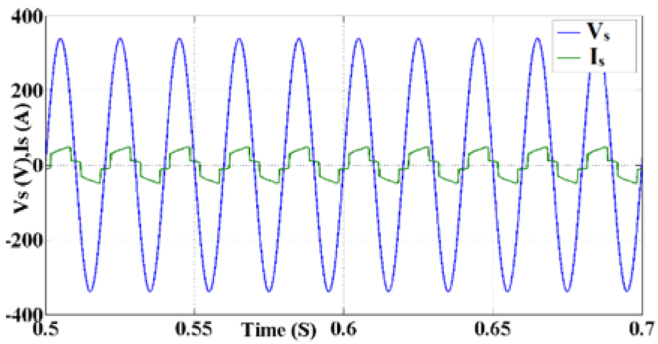

Figure 15. Power factor at source without compensation

3.2. Analysis of wind energy system with simple hysteresis current controller

Now, the WES with STATCOM and SHCC is simulated, and the waveforms are shown in Figure 16. The load current waveform in Figure 16(a) is non-sinusoidal. From Figure 16(b), it is clear that the source current is sinusoidal, as the STATCOM is injecting currents to cancel out harmonics. It is indicated in Figure 17 that the source current has an acceptable THD value due to STATCOM and its controller. As can be seen from Figure 18, the power factor at the source is UPF due to the presence of STATCOM and its controller.

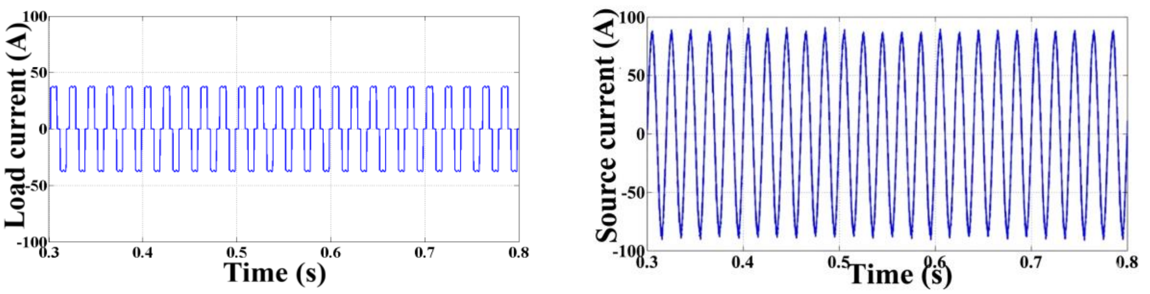

(a) (b)

Figure 16. Current waveforms of the grid-connected WES with SHCC-based STATCOM: (a) nonlinear load current waveform and (b) source current waveform with improved sinusoidal behavior due to compensation

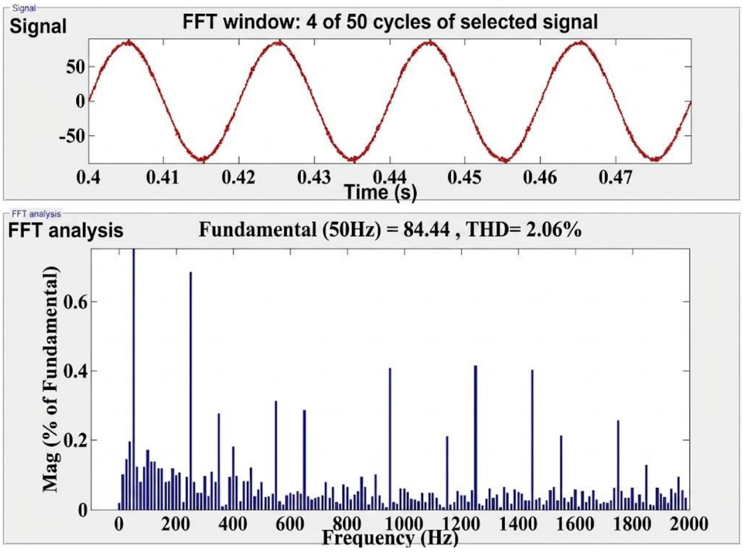

Figure 17. THD value of source current with SHCC

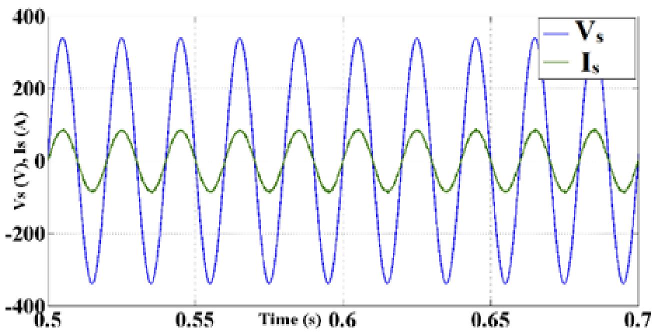

Figure 18. Power factor at source with SHCC

3.3. Analysis of wind energy system with space vector hysteresis current controller

Now, WES with STATCOM and SVHCC is simulated, and the waveforms are shown in Figure 19. The load current waveform in Figure 19(a) is non-sinusoidal. From Figure 19(b), it is clear that the source current is sinusoidal, as the STATCOM is injecting currents to cancel out harmonics. It is indicated in Figure 20 that the source current has an accepted value of THD of 1.52%, due to STATCOM and its controller. As can be seen from Figure 21, the power factor at the source is UPF due to the presence of STATCOM and its controller.

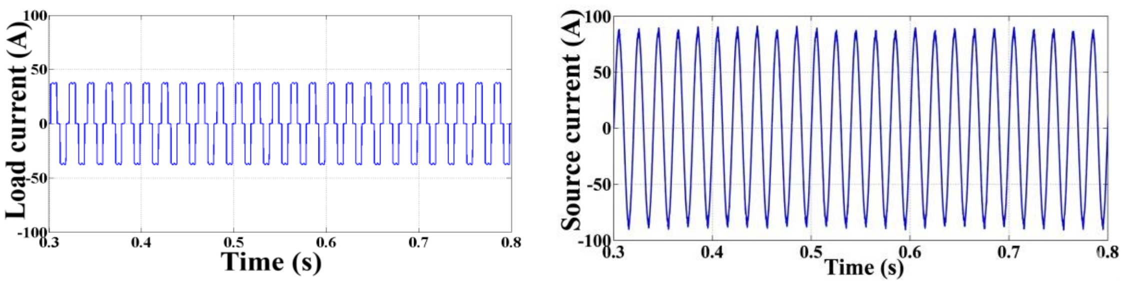

(a) (b)

Figure 19. Current waveforms of the grid-connected WES with SVHCC-based STATCOM: (a) nonlinear load current waveform and (b) source current waveform with near-sinusoidal behavior

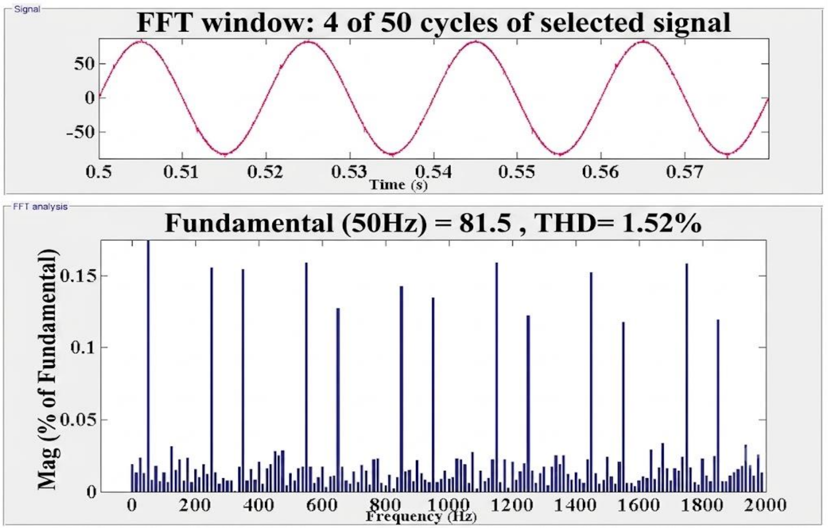

Figure 20. THD value of source current with SVHCC

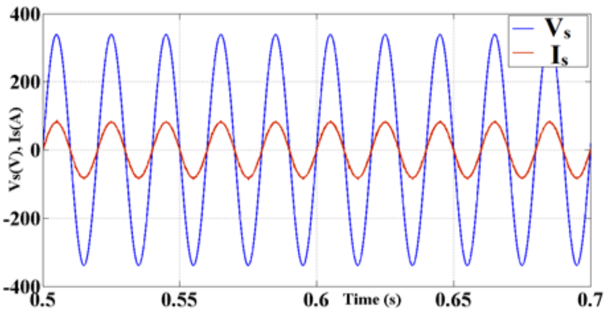

Figure 21. Power factor at source with SVHCC

3.4. Analysis of SHCC and SVHCC regarding switching frequency

The use of appropriate VVs, as outlined in the switching tables in Tables 2 and 3, is expected to result in a lower operating frequency for SVHCC compared to SHCC. In SHCC, there is no systematic way of using a switching table for switching IGBTs of STATCOM, and it is supposed to operate at a higher frequency. Figure 22 shows the variation in switching frequency of the IGBT in STATCOM for both SHCC and SVHCC controllers, which helps to prove this fact. It is clear from Figure 22(a) that the IGBT of SHCC is operating at 100 kHz, whereas in Figure 22(b) the IGBT of SVHCC is operating at 50 kHz.

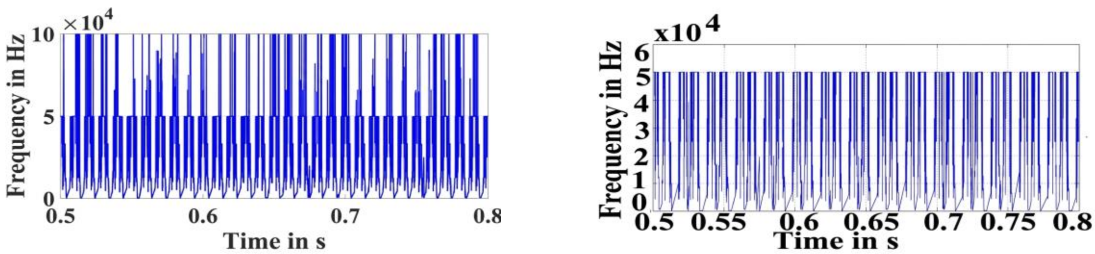

(a) (b)

Figure 22. Switching frequency plots: (a) SHCC and (b) SVHCC

Dash *et al*. [30] report compensated grid current THD values of 3.66%, 4.56%, and 3.92%, with variations between 2.7%–4.9% under transient conditions. Gadupudi *et al.* [31] report a THD of 3.74% for a seven-level VSC-based STATCOM, whereas the proposed method attains 1.52%, indicating improved PQ and efficiency. Gopinath *et al.* [32] report that optimization techniques such as modified non-dominated sorting genetic algorithm and salp swarm algorithm obtain a THD of about 2.14% for a 15-level inverter. Compared to these computationally intensive methods, the proposed SVHCC controller achieves a lower THD of 1.52% with reduced switching frequency and simpler implementation, making it more suitable for practical grid-connected WES.

4. CONCLUSION

In this proposed research study, multilevel inverter-based STATCOM with SVHCC is simulated using MATLAB/Simulink. To highlight the effectiveness of SVHCC, a comparative study is made without a controller and then with SHCC controller-based STATCOM. The research has achieved its objective of enhancing PQ in grid-connected WES using multilevel inverter-based STATCOM with SVHCC. The proposed approach successfully addressed the major difficulties such as harmonic distortion and poor power factor associated with nonlinear loads and IGs. The fundamental contribution of this work is the coordinated SVHCC control approach, which improves current regulation and the switching frequency with respect to the conventional methods. The suggested system shows a considerable performance increase, such as reducing the THD from 26.12% to 1.52%, achieving UPF, and reducing the switching frequency from 100 kHz to 50 kHz compared to the SHCC-based approach. The results demonstrate that the proposed SVHCC-based STATCOM is an effective and dependable option for PQ improvement in renewable energy integrated grids. This has significant practical consequences for enhancing grid stability, lowering stress on power electronic devices, and enabling more effective large-scale integration of WESs. Future work can be a real-time implementation of the proposed controller using a laboratory-scale prototype with digital signal processor (DSP)/field programmable gate array (FPGA) controllers. Hardware-in-the-loop (HIL) testing can be implemented to authenticate performance under realistic grid disturbances. The performance can be further assessed under severe grid conditions such as voltage sag/swell, unbalanced faults, and frequency deviations. This shall prove the robustness of the proposed controller in weak and disturbed grid environments. The suggested controller has the capability to be scaled up for higher power ratings and can also accommodate different multilevel inverter configurations, including modular multilevel converter (MMC) designs. A comparative analysis involving various topologies will provide design strategies tailored for large-scale WESs. Future investigations may incorporate adaptive tuning or advanced methodologies such as fuzzy logic, neural networks, or model predictive control to dynamically modify hysteresis bands and optimize space vector selection.

FUNDING INFORMATION

Authors state no funding involved.

AUTHOR CONTRIBUTIONS STATEMENT

This journal uses the Contributor Roles Taxonomy (CRediT) to recognize individual author contributions, reduce authorship disputes, and facilitate collaboration.

Name of Author	C	M	So	Va	Fo	I	R	D	O	E	Vi	Su	P	Fu
Gundala Muni Reddy	✓	✓	✓	✓	✓	✓		✓	✓	✓		✓	✓	
Ammapalli Hema Sekhar		✓		✓		✓	✓	✓	✓		✓			✓
Selika Narasimha Rao	✓	✓	✓	✓	✓	✓	✓	✓		✓	✓	✓	✓	✓
Kuruna Divakar		✓		✓		✓	✓		✓	✓			✓	✓
Kola Murali Kumar	✓				✓			✓		✓		✓	✓	
Nathella Munirathanm Giri Kumar	✓		✓		✓		✓		✓					✓
Gunti Kishor Babu		✓		✓	✓		✓			✓		✓		✓
Vayyala Jyothsna Priya	✓		✓			✓		✓		✓	✓			✓

C : **C**onceptualization
M : **M**ethodology
So : **So**ftware
Va : **Va**lidation
Fo : **Fo**rmal analysis
I : **I**nvestigation
R : **R**esources
D : **D**ata Curation
O : Writing - **O**riginal Draft
E : Writing - Review & **E**diting
Vi : **Vi**sualization
Su : **Su**pervision
P : **P**roject administration
Fu : **Fu**nding acquisition

CONFLICT OF INTEREST STATEMENT

Authors state no conflict of interest.

DATA AVAILABILITY

The data that support the findings of this study are available from the corresponding author, [GMR], upon reasonable request.

REFERENCES

[1] M. Santamouris and K. Vasilakopoulou, "Present and future energy consumption of buildings: challenges and opportunities towards decarbonisation," *e-Prime - Advances in Electrical Engineering, Electronics and Energy*, vol. 1, 2021, doi: 10.1016/j.prime.2021.100002.

[2] I. Dincer and A. A. Rayash, "Energy sources," in *Energy Sustainability*, Amsterdam, Netherland: Elsevier, 2020, pp. 19–58, doi: 10.1016/B978-0-12-819556-7.00002-4.

[3] C. R. J. Kumar and M. A. Majid, "Renewable energy for sustainable development in India: current status, future prospects, challenges, employment, and investment opportunities," *Energy, Sustainability and Society*, vol. 10, no. 1, p. 2, Dec. 2020, doi: 10.1186/s13705-019-0232-1.

[4] J. G. Speight, "Current fuel sources and alternate fuel sources," in *Chemistry and Technology of Alternate Fuels*, Singapore: World Scientific, 2020, pp. 3–61, doi: 10.1142/9789811203657_0001.

[5] T. Kober, H. W. Schiffer, M. Densing, and E. Panos, "Global energy perspectives to 2060 – WEC's world energy scenarios 2019," *Energy Strategy Reviews*, vol. 31, Sep. 2020, doi: 10.1016/j.esr.2020.100523.

[6] S. Dey, A. Sreenivasulu, G. T. N. Veerendra, K. V. Rao, and P. S. S. A. Babu, "Renewable energy present status and future potentials in India: an overview," *Innovation and Green Development*, vol. 1, no. 1, Sep. 2022, doi: 10.1016/j.igd.2022.100006.

[7] A. Dani, M. Benlamlih, Z. Mekrini, M. El Mrabet, and M. Boulaala, "Wind energy conversion technologies and control strategies: a review," *International Journal of Renewable Energy Research*, vol. 14, no. 1, 2024.

[8] T. Bjärstig, I. Mancheva, A. Zachrisson, W. Neumann, and J. Svensson, "Is large-scale wind power a problem, solution, or victim? a frame analysis of the debate in Swedish media," *Energy Research and Social Science*, vol. 83, Jan. 2022, doi: 10.1016/j.erss.2021.102337.

[9] S. Meda, B. P. Muni, and K. R. Reddy, "An intelligent mechanism for enhancing power quality in grid-tied DFIG based wind energy system using simplified vector-controlled statcom," *International Journal of Intelligent Systems and Applications in Engineering*, vol. 12, no. 1s, pp. 106–116, 2024.

[10] O. P. Mahela, B. Khan, H. H. Alhelou, and S. Tanwar, "Assessment of power quality in the utility grid integrated with wind energy generation," *IET Power Electronics*, vol. 13, no. 13, pp. 2917–2925, Oct. 2020, doi: 10.1049/iet-pel.2019.1351.

[11] S. A. Almohaimeed and M. A. Akher, "Power quality issues and mitigation for electric grids with wind power penetration," *Applied Sciences*, vol. 10, no. 24, Dec. 2020, doi: 10.3390/app10248852.

[12] T. Ravi, K. S. Kumar, C. Dhanamjayulu, B. Khan, and K. Rajalakshmi, "Analysis and mitigation of PQ disturbances in grid connected system using fuzzy logic based IUPQC," *Scientific Reports*, vol. 13, no. 1, 2023, doi: 10.1038/s41598-023-49042-z.

[13] G. Vineeth, J. L. Aishwarya, B. Sowmya, B. S. Rani, and M. Narasimha, "Power quality enhancement in grid-connected renewable energy sources using MC-UPQC," in *2023 International Conference on Power, Instrumentation, Energy and Control*, Feb. 2023, pp. 1–6, doi: 10.1109/PIECON56912.2023.10085824.

[14] K. Chahine, M. Tarnini, N. Moubayed, and A. El Ghaly, "Power quality enhancement of grid-connected renewable systems using a matrix-pencil-based active power filter," *Sustainability*, vol. 15, no. 1, Jan. 2023, doi: 10.3390/su15010887.

[15] T. Magesh, G. Devi, and T. Lakshmanan, "Measurement and simulation of power quality issues in grid connected wind farms," *Electric Power Systems Research*, vol. 210, Sep. 2022, doi: 10.1016/j.epsr.2022.108142.

[16] H. Shao, R. Henriques, H. Morais, and E. Tedeschi, "Power quality monitoring in electric grid integrating offshore wind energy: a review," *Renewable and Sustainable Energy Reviews*, vol. 191, Mar. 2024, doi: 10.1016/j.rser.2023.114094.

[17] X. Pan, L. Zhang, Y. Li, K. Li, and H. Huang, "Modulated model predictive control with branch and band scheme for unbalanced load compensation by MMCC-STATCOM," *IEEE Transactions on Power Electronics*, vol. 37, no. 8, pp. 8948–8962, Aug. 2022, doi: 10.1109/TPEL.2022.3152407.

[18] C. M. Martín, S. Arnaltes, F. Arredondo, J. A. Martínez, and J. L. R. Amenedo, "Increasing grid access capacity for renewable integration through a grid-forming E-STATCOM under Spanish regulation," *Renewable Energy Focus*, vol. 56, Mar. 2026, doi: 10.1016/j.ref.2025.100786.

[19] A. Benevieri, S. Cosso, A. Formentini, M. Marchesoni, M. Passalacqua, and L. Vaccaro, "Advances and perspectives in multilevel converters: a comprehensive review," *Electronics*, vol. 13, no. 23, Nov. 2024, doi: 10.3390/electronics13234736.

[20] S. J. Yeboah, S. Nunoo, J. C. Attachie, W. D. Asihene, and E. Y. Asuamah, "Impact and integration techniques of renewable energy sources on smart grid operations: a systematic review," *Scientific African*, vol. 29, 2025, doi: 10.1016/j.sciaf.2025.e02845.

[21] S. S. S. R. S. Duvvuri, V. Sandeep, K. Yadlapati, and V. B. M. Krishna, "Research on induction generators for isolated rural applications: state of art and experimental demonstration," *Measurement: Sensors*, vol. 24, Dec. 2022, doi: 10.1016/j.measen.2022.100541.

[22] M. A. Khlifi and M. B. Slimene, "Efficiency of a six-phase induction generator employing a static excitation controller to generate AC power for wind energy," *IEEE Access*, vol. 11, pp. 28791–28799, 2023, doi: 10.1109/ACCESS.2023.3260775.

[23] E. Madhurima, P. S. Puhan, and K. Sumanth, "Performance analysis of photovoltaic fed series active power filter for power quality improvement," in *2020 3rd International Conference on Energy, Power and Environment: Towards Clean Energy Technologies*, Mar. 2021, pp. 1–6, doi: 10.1109/ICEPE50861.2021.9404501.

[24] Y. V. P. Kumar *et al.*, "Fuzzy hysteresis current controller for power quality enhancement in renewable energy integrated clusters," *Sustainability*, vol. 14, no. 8, Apr. 2022, doi: 10.3390/su14084851.

[25] M. Mukherjee and A. Banerjee, "Power quality improvement by active shunt filter with hysteresis current controller," in *Advances in Communication, Devices and Networking*, Singapore: Springer Nature, 2019, pp. 89–97, doi: 10.1007/978-981-13-3450-4_11.

[26] R. S. R. Sankar, A. Venkatesh, and D. Kollipara, "Adaptive hysteresis band current control of grid connected PV inverter," *International Journal of Electrical and Computer Engineering*, vol. 11, no. 4, pp. 2856–2863, Aug. 2021, doi: 10.11591/ijece.v11i4.pp2856-2863.

[27] R. Qin, H. Kuang, H. Jiang, H. Yu, H. Li, Z. Li, "Improved sequential model predictive control of cascaded H-bridge multilevel converter," *IEEJ Transactions on Electrical and Electronic Engineering*, vol. 19, pp. 1046–1059, Feb. 2024, doi: 10.1002/tee.24043.

[28] K. Biju and R. Ramchand, "A new space vector pulse width modulation technique for single-phase seven-level inverter with reduced number of switches," *IETE Journal of Research*, vol. 68, no. 3, pp. 1661–1674, May 2022, doi: 10.1080/03772063.2019.1664339.

[29] S. Bhatnagar, S. Tiwari, T. Mahawar, S. Pancholi, and B. Modi, "Space-vector modulation of a three-level NPC-inverter," *International Research Journal of Engineering and Technology*, vol. 8, no. 7, pp. 4846–4850, 2021.

[30] A. Dash *et al.*, "Grid-tied distribution static synchronous compensator for power quality enhancement using combined-step-size real-coefficient improved proportionate affine projection sign algorithm," *Energies*, vol. 15, no. 1, Dec. 2021, doi: 10.3390/en15010197.

[31] L. N. Gadupudi, G. S. Rao, R. Devarapalli, and F. P. G. Márquez, "Seven-level voltage source converter based static synchronous compensator with a constant DC-link voltage," *Applied Sciences*, vol. 11, no. 16, Aug. 2021, doi: 10.3390/app11167330.

[32] B. Gopinath, S. Suresh, G. Jayabaskaran, and M. Geetha, "Renewable energy resource integrated multilevel inverter using evolutionary algorithms," *Automatika*, vol. 65, no. 3, pp. 1061–1078, 2024, doi: 10.1080/00051144.2024.2329494.

BIOGRAPHIES OF AUTHORS

Dr. Gundala Muni Reddy received Ph.D. degree from S.V. University, Tiruapati, India and M.Tech. in Computer Applications in Industrial Drives from Visvesvaraya Technological University, Belgaum, Karnataka, India and B.Tech. degree in Electrical Engineering from Jawaharlal Nehru Technological University Hyderabad, Andhra Pradesh, India. His research interests include the power electronics, PQ, and renewable energy. He is at present working with Department of Electrical and Electronics Engineering, Siddharth Institute of Engineering and Technology, Puttur, India. He can be contacted at email: munireddyg@gmail.com.

Dr. Ammapalli Hema Sekhar received his B.Tech. degree in Electrical and Electronics Engineering from Jawaharlal Nehru Technological University Hyderabad, at Sree Vidyanikethan Engineering College, Andhra Pradesh. He received of M.Tech. and Ph.D. from S.V. University College of Engineering, Tirupati. His areas of interest are power systems, distribution systems, electrical machines, power system stability and control, and power system optimizations. He is at present working with Department of Electrical and Electronics Engineering, VEMU Institute of Technology, Kothakota, India. He can be contacted at email: ahemasekar@gmail.com.

Dr. Selika Narasimha Rao received his B.Tech. degree from S.V. College of Engineering, S.V. University in 2004 and M.E degree from Sathyabama University Chennai, India in 2010, and Ph.D. degree from Pondicherry Central University, Puducherry, India in the year 2023. His areas of interest are of partial discharge, motor windings insulation, and modeling of insulation. He is at present working with Department of Electrical and Electronics Engineering, Siddharth Institute of Engineering and Technology, Puttur, India. He can be contacted at email: snrinskit@gmail.com.

Dr. Kuruna Divakar received Ph.D. degree in control and automation from Vellore Institute of Technology, Vellore, India, and M.Tech. in power electronics from Jawaharlal Nehru Technological University Anantapur, Andhra Pradesh, and B.Tech. degree in Electrical Engineering from Jawaharlal Nehru Technological University Hyderabad, Andhra Pradesh, India. His research interests include the areas of process dynamic control and system theory. He is at present working with Department of Electrical and Electronics Engineering, Siddharth Institute of Engineering and Technology, Puttur, India. He can be contacted at email: divakar.kumara@gmail.com.

Dr. Kola Murali Kumar received the B.Tech. degree in Electrical and Electronics Engineering from Jawaharlal Nehru Technological University Hyderabad, India, in 2006, M.Tech. degree in Power Electronics and Electrical Drives from Jawaharlal Nehru Technological University Anantapur, India, in 2013, and received Ph.D. in Power Electronics from Vellore Institute of Technology, Vellore, India, in 2022. His research interests include MLIs, power converters, fuzzy and ANFIS controllers. He is at present working with Department of Electrical and Electronics Engineering, Siddharth Institute of Engineering and Technology, Puttur, India. He can be contacted at email: kolamuralikumar@gmail.com.

Dr. Nathella Munirathanm Giri Kumar has obtained his B.E. in Electrical and Electronics Engineering from Sir M. Visvesvaraya Institute of Technology, Bangalore, and his M.Tech. and Ph.D. from SV University, Tirupati. Areas of interest are power system planning, security, and state estimation; reliability studies; and real-time application of power system studies with artificial intelligence and machine learning concepts. He can be contacted at email: nmgkumar@gmail.com.

Dr. Gunti Kishor Babu received the B.Tech. degree in Electrical and Electronics Engineering from Jawaharlal Nehru Technological University Hyderabad, India, in 2006; M.Tech. degree in Power Electronics and Electric Drives from Jawaharlal Nehru Technological University Hyderabad, India, in 2008; and received Ph.D. in Control Systems from Acharya Nagarjuna University, Guntur, Andhra Pradesh, India, in 2017. He has published more than 31 articles in international/national journals and conferences. His research interests include power converters, singular perturbation methods, optimal control, electric vehicles, and machine learning. He is at present working with Department of Electrical and Electronics Engineering, Kallam Haranadhareddy Institute of Technology, Guntur, India. He can be contacted at email: kish.eee01@gmail.com.

Vayyala Jyothsna Priya received the B.Tech. degree in Electrical and Electronics Engineering from Jawaharlal Nehru Technological University Hyderabad, India, in 2006 with the university's fifth rank; M.Tech. degree in Electrical Power Systems from Jawaharlal Nehru Technological University Anantapur, India, in 2012 with gold medal. Her research interests include PQ, renewable energy, electric vehicles, and machine learning. She is at present working with Department of Electrical and Electronics Engineering, Siddharth Institute of Engineering and Technology, Puttur, India. She can be contacted at email: jyothsnavayyala@gmail.com.